Accelerated maturation of white matter in young children with autism: A high b value DWI study

Dafna Ben Bashat,[a,*] Vered Kronfeld-Duenias,[a,b] Ditza A. Zachor,[c,d] Perla M. Ekstein,[e] Talma Hendler,[a,d] Ricardo Tarrasch,[f] Ariela Even,[g] Yonata Levy,[g,h] and Liat Ben Sira[a]

[a]Functional Brain Mapping Unit, The Wohl Institute for Advanced Imaging, Tel Aviv Sourasky Medical Center, 6 Weizamnn st. Tel Aviv, 64239, Israel
[b]The Lester and Sally Entin Faculty of Humanities, Tel Aviv University, Tel Aviv, Israel
[c]Department of Pediatric, Autism Center, Assaf Harofe Medical Center, Israel
[d]Sackler Faculty of Medicine, Tel Aviv University, Tel Aviv, Israel
[e]Department of Anesthesia and Critical Care, Tel Aviv Sourasky Medical Center, Tel Aviv, Israel
[f]Department of Psychology, Tel Aviv University, Tel Aviv, Israel
[g]Psychology Department, The Hebrew University, Jerusalem, Israel
[h]Hadassah-Hebrew University Medical School, Jerusalem, Israel

The goal of this work was to study white matter maturation in young children with autism following previous reports of increased cerebral volume during early development, as well as arguments for abnormal neural growth patterns and regulation at this critical developmental period. We applied diffusion tensor imaging (DTI) and high b value diffusion-weighted imaging (DWI) to young children diagnosed with autism and to a typically developing (TD) control group. Fractional anisotropy (FA), probability and displacement were measured in overall analysis as well as in regions of interest (ROI). Individual data points of children with autism were compared to the developmental curves obtained from typically developing children. Increased restriction, reflected in significantly increased FA and probability along with reduced displacement values, was detected in overall analysis as well as in several brain regions. Increased restriction, suggesting an early and accelerated abnormal maturation of white matter, was more dominant in the left hemisphere and was mainly detected in the frontal lobe. No changes were detected in the occipital lobes. These results support previous claims of abnormal brain overgrowth in young children with autism and are in contrast to the decreased restricted diffusion reported in previous studies in adolescent with autism.
© 2007 Elsevier Inc. All rights reserved.

Introduction

The goal of this work was to study white matter maturation in young children with autism using DTI (diffusion tensor imaging) and high b value DWI (diffusion-weighted imaging). Autism is a

common neurodevelopmental disorder affecting about 1:1000 children. Up to 6:1000 children have some form of the disorder that is within the autistic spectrum disorder (ASD) (Fombonne, 2003). Within ASD, there is variability in the level of functioning and 40–75% of the children are mentally retarded (Ben-Itzchak and Zachor, 2007; Bertrand et al., 2001; Fombonne, 2003).

In the absence of specific laboratory tests, autism is diagnosed on the basis of behavioral criteria in three key domains: reciprocal social interaction, language and communication and restricted/repetitive behaviors. Diagnosis of autism is usually made around the age of 18–24 months, although parents typically report concerns in the first year of life. This gap between parents' early concerns and the relatively late diagnosis, along with the importance of early intervention, highlight the necessity to find a reliable tool for early diagnosis, possibly through identification of brain abnormalities.

One of the common assumptions regarding brain abnormalities in autism relates to the rate of brain growth. Studies dealing with this issue used head circumference measurements, imaging and postmortem methods. These studies suggest that autism is a disorder that involves a transient period of postnatal brain overgrowth. At birth, brain size in autism is equivalent or slightly smaller than the normal average and the rate of macrocephaly is low relative to control groups. However, abnormally accelerated brain growth is observed in 70% of children with autism during the first 2 years of life (Courchesne and Pierce, 2005; Lainhart, 2006; Penn, 2006; Redcay and Courchesne, 2005). It was suggested that this acceleration results in dramatic increase in brain size and a four time increase in macrocephaly during those years. In later childhood years, brain growth is slowed or arrested and later plateaus, so that in adolescence and in adulthood brain size in autism is not significantly different from the healthy average.

---

* Corresponding author. Fax: +972 3 6973080.
  E-mail address: dafnab@tasmc.health.gov.il (D. Ben Bashat).
  Available online on ScienceDirect (www.sciencedirect.com).

Imaging studies suggest excessive cerebral growth of both white and gray matter in autism, especially in the frontal lobes. Studies reported smaller volumes of the cerebellar vermis (Akshoomoff et al., 2004; Carper and Courchesne, 2005; Carper et al., 2002; Courchesne et al., 2001), as well as abnormalities in the amygdalae and hippocampi in children with autism, ages 3–4 years (Sparks et al., 2002). Additionally, histological analyses of brains of children and adults with autism showed more numerous, smaller and less compact cell columns in Brodmann frontal area 9 and temporal areas 21 and 22 (Casanova et al., 2002a,b).

Abnormal structure of the gray matter, such as reported above, may be related to malformations of the white matter. The study of the latter is especially intriguing in autism considering the fact that the cognitive deficit in autism is most likely to arise when the task requires integrative processing. Such processes involve intrahemispheric as well as interhemispheric transfer of information which has been found to be abnormal in autism (Just et al., 2004; Minshew et al., 1997).

Estimation of white matter using imaging techniques is more accurately performed through diffusion tensor imaging (DTI) ((Engelbrecht et al., 2002; Mukherjee and McKinstry, 2006; Neil et al., 2002). DTI provides three valuable parameters: (1) the average extent of water diffusion (apparent diffusion constant—ADC) which provides information on restriction and boundaries (high packing density of cells); (2) the fractional anisotropy (FA) that is higher in dense and ordered structure; and (3) the orientation of the ordered structure (color coded DTI).

To date, few studies have used DTI in autism and in ASD. Barnea-Goraly et al. (2004) reported reductions in FA in high functioning adolescents with autism, ages 11–18 years, in brain regions related to social cognition such as the ventromedial prefrontal cortices, the anterior cingulate gyri and the temporoparietal junction. Other studies which have studied adolescence with autism reported reduced FA along with reduced volume and increased diffusion in the corpus callosum (Alexander et al., 2007), reduced FA values in the thalamus (Lazar et al., 2006) and reduced FA in the following: left corona radiate near the genu of the corpus callosum, bilateral areas near the splenium of the corpus callosum, areas of the left frontal white matter near Broca's area, posterior bilateral areas of the inferior fronto-occipital fasciculus and bilateral areas of superior longitudinal fasciculus (Keller et al., 2006). Overall the above results suggest less structural integrity of white matter in subjects during late childhood or during the second decade of life. In contrast, a recent study found significantly higher ADC values in the arcuate fasciculus in children with autism less than 3.5 years of age (Williams et al., 2006). However, no changes in FA were reported in that work.

The current study applied conventional DTI along with the related, recently introduced high b value diffusion-weighted imaging (DWI) to study white matter maturation and pathophysiology in young children with autism. Whereas conventional DTI uses images acquired at low b values of about 1000 s/mm^2 that are believed to measure diffusion in the less restricted compartments, high b value DWI uses images acquired at b values above 3000 s/mm^2 in which the diffusion component originates mainly from more restricted compartments, i.e. the axonal milieu (Assaf and Cohen, 2000). Assuming that myelination and pathology of white matter are more likely to be detected in restricted compartments, high b value DWI is likely to be a sensitive method of such processes. Indeed, while conventional MRI show developmental changes mainly up to 2 years of age, FA showed changes in white matter in healthy children up to 6–8 years of age or less (Hermoye et al., 2006; McGraw et al., 2002; Mukherjee et al., 2002), and high b value method demonstrated changes throughout adulthood (Ben Bashat et al., 2005). Moreover, previous studies showed that in multiple sclerosis, vascular dementia, adrenoleukodystrophy and schizophrenia, probability (Prob) and displacement (Disp), calculated through high b value DWI, were better indicators of white matter pathology than the conventional FA (Assaf et al., 2002a,b; Ben-Bashat et al., 2003, 2004; Mendelsohn et al., 2006). In view of the above, the focus in the current study will be on Prob and Disp, with FA serving as a complimentary data source.

In the current study, DTI and high b value DWI were applied to young children with autism and to typically developing children. We hypothesized that at an early age there will be an increase in restriction of white matter in children with autism, reflecting abnormal maturation of white matter. Such increase may explain the converging evidence of brain enlargement in early childhood and support the claim of abnormal pruning in children with autism.

Methods

Participants

Study group

The protocol was applied to seventeen children with autism. The current report is confined to the seven youngest children, ages 1.8–3.3, which is the age range for which accelerated brain growth and dramatic brain enlargement have been observed (Courchesne and Pierce, 2005; Lainhart, 2006; Penn, 2006; Redcay and Courchesne, 2005). All the children met the cut-off points for autism on the Autism Diagnosis Interview-Revised, ADI-R (Lord et al., 1994, 2000) as well as on the Diagnostic Observational Schedule Generic, ADOS (Lord et al., 1999) and fulfilled DSM-IV criteria for autism. All children were re-evaluated on the ADOS 2 years after the MRI examination and diagnosis of autism was confirmed. In addition, participants underwent a complete neuropediatric and cognitive assessment. Children with neurological co-morbidities were excluded from the study.

Control group

Forty-one MR scans were acquired from TD subjects (18 boys), ages 4 months to 23 years, mean age 9.6. Subjects up to age 10 years were referred for suspected neurological abnormalities. Subjects 10 years and older were recruited specifically for this study. Requirements for eligibility were the following: normal developmental history, attendance of a regular school, no history of seizures or head injury, no clinical evidence of neurological dysfunction and normal imaging as judged by a clinical neuroradiologist. Participants or their legal guardians signed an informed consent form. The Institutional Review Board (IRB) of the Tel-Aviv Medical Center and the Israeli Ministry of Health approved the MRI and sedation protocols detailed below.

Sedation protocol

When necessary, participants under the age of 10, underwent sedation with a gas mixture of nitrous oxide in 40% oxygen enriched with halothane 0.6–0.8%. Subjects breathed spontaneously through a laryngeal mask airway. EKG, pulse oximetry

and capnography were monitored. Cooperative participants were scanned without sedation.

Image acquisition

MRI was performed on a 1.5-T GE Signa Horizon, Echo speed, LX MRI scanner (Milwaukee, WI, USA). The protocol included anatomical sequences—Sagittal T_1 and Axial T_2, weighted images as well as Axial FLAIR and Coronal T_2. The diffusion images (used for both DTI and q-space) were obtained from a series of 8 diffusion gradients with a maximum b value of 6000 s/mm^2, performed at 6 non-collinear gradient directions. Other experimental parameters were TR/TE$=1800/128$ ms, $\Delta/\delta=52.5/47$ ms, effective maximal gradient strength of 3.11 gauss/cm and averages of 4 measurements. Each volume consisted of four slices, 4.5-mm thickness with in-plane resolution of 1.87×1.87 mm, FOV$=240$ mm and were acquired parallel to the AC-PC line, from the corpus callosum up to the subcortical white matter. Total acquisition time for both diffusion scans was 5:34 min.

Data analysis

Three sets of images were extracted from the same DWI scan— FA, Prob and Disp. FA maps were calculated from thirty-one volumes acquired at different low b values (up to 1104 s/mm^2). For each voxel, the diffusion tensor (i.e., a 3×3 matrix) was calculated with a multivariate linear fitting algorithm (Basser et al., 1994). The tensor in each voxel was spectral decomposed to obtain its eigenvalues and eigenvectors, and the fiber direction at each voxel was assumed to be the eigenvector corresponding to the tensor's largest eigenvalue. This vector was color-coded (blue for superior–inferior, red for left–right and green for anterior–posterior), with a brightness proportional to the voxel's FA (Pajevic and Pierpaoli, 1999). Prob and Disp maps were obtained, using q-space analysis for the entire diffusion data set, as described in our previous papers (Assaf et al., 2002a; Ben-Bashat et al., 2003, 2005). Briefly, in each pixel, the signal decay which is a function of the q values (defined as $\gamma\delta g/2\pi$) was first zero filled to 128 data points. Fourier transform was then applied to produce the displacement distribution profile. The maximum intensity of the peak and the full width at half height functions were extracted to produce Prob (measured in arbitrary units: a.u.) and Disp (measured in micrometers: µm) images.

Fig. 1 shows axial images of a 22-year-old healthy participant: T_1-weighted image (1A), FA map (1B), Prob map (1C) and Disp map (1D). As can be seen in Fig. 1B, the brightness is proportional to the voxel's FA, and ordered structures such as the white matter have high FA values. In Figs. 1C and D, the white matter shows high probability and low displacement values.

FA and q-space values were analyzed with in-house software written in Matlab$^©$. Overall white matter pixels count (WMPC) and region of interest analyses (ROI) were performed on the three calculated indices (FA, Prob and Disp). In the first analysis, the number of pixels representing mature white matter was calculated for each subject from a histogram averaged on all acquired slices. The chosen values of mature white matter were between 0.256 and 0.9 for the FA histograms, between 3.75 and 8.0 a.u. for the Prob and between 2.2 and 7.2 µm for the Disp histograms. Values were chosen based on images of adult parti-cipants since they provided clearer segmentation of the white matter.

In the second analysis, quantitative region of interest (ROI) measurements were performed in 18 anatomical regions in the brain, shown on Figs. 2A–D. Regions of white matter were manually prescribed on color-coded DTI, segmenting the fibers according to directions. ROIs were selected according to the MRI Atlas of Human White Matter and were labeled in the conventional way (Mori et al., 2005). It is important to note, however, that in our study the total brain volume was not acquired and so the ROIs represent only parts of the fibers after which they are named. In order to evaluate the precision of the manual selection, ROIs were prescribed by a second experimenter on a random selection of scans. Between-judge reliability, as measured by Pearson correla-tions, was 0.9.

ROIs were prescribed separately for each hemisphere and when possible, defined on more than one slice. The ROIs were genu of the corpus callosum (gcc), splenium of the corpus callosum (scc), anterior limb of the internal capsule (alic), posterior limb of the internal capsule (plic), external capsule (ec), forceps minor (fminor) and forceps major (fmajor), cortico-spinal tract (cst) and the superior longitudinal fasciculus (slf). Averaged values of FA, Prob and Disp were computed for each ROI for each subject. ROI selection of the slf area, however, was not possible in two children, and therefore average values for the slf are based on five children.

A mono-exponential function with least squares curve fitting ($y=a_1+a_2{}^{*}\exp(age/a_3$, where y stands for FA/Prob/Disp values) was used to produce developmental curves from the data points of the control group (Ben Bashat et al., 2005). The data points for the children with autism were plotted against these curves. Mean values of the study group were compared to the mean values
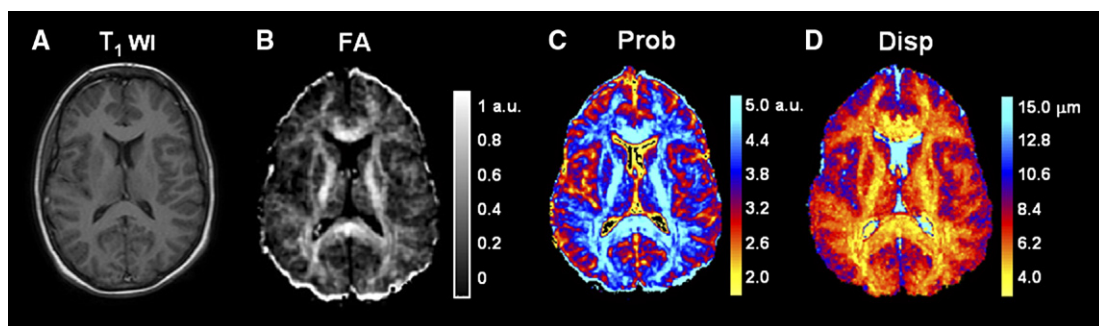

Fig. 1. T_1-weighted images (T_1-WI-A), fractional anisotropy (B), probability (C) and displacement (D) in a 22-year-old healthy participant. Fractional anisotropy and probability values are measured in arbitrary units (a.u.), displacement is measured in micrometers (µm).
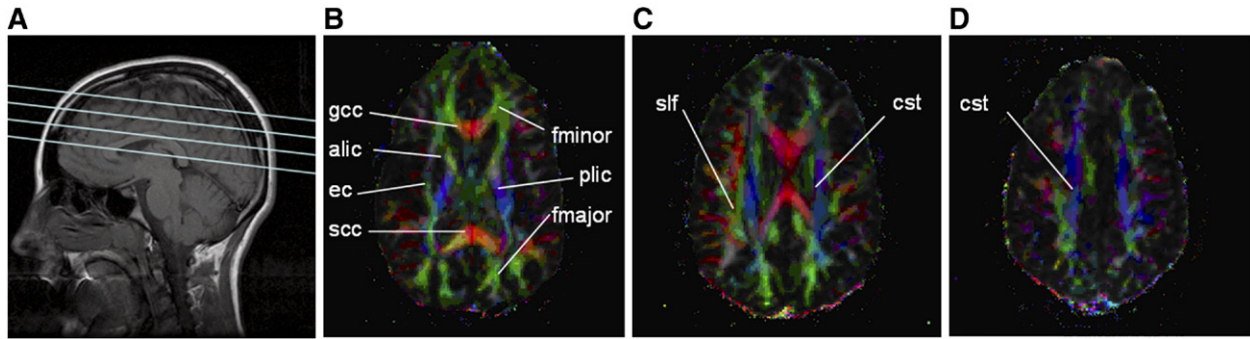
Fig. 2. Sagittal image of the brain, with lines representing the location of the acquired slices (A). Selected ROIs prescribed on color coded DTI (B–D). Different slices are shown in the images. Colors represent directions: blue for superior–inferior, red for left–right, and green for anterior-posterior. gcc: genu of the corpus callosum; scc: splenium of the corpus callosum; alic: anterior limb of the internal capsule; plic: posterior limb of the internal capsule; ec: external capsule; slf: superior longitudinal fasciculus; fminor: forceps minor; fmajor: forceps major.

predicted by the developmental curves for age-matched healthy controls. One sample, one-tail t-tests were performed ($p<0.05$) to evaluate the differences between the values obtained for children with autism and the predicted normal values for the overall analysis. For the ROIs analyses, Keppel multiple comparisons correction for 18 regions was applied ($p<0.033$).

Results

Conventional MR imaging

Children with autism demonstrated normal gray white matter differentiation, normal midline structures including the corpus callosum, cavum septum pellucidum, pituitary gland and chiasm, normal cerebellum, vermis and cranio-cervical junction. In five out of seven children with autism, mild increased periventricular signal at the level of the atrium was noted on the FLAIR images, representing terminal myelinization which is likely a normal variant. None of the patients demonstrated cortical dysgenesis.

White matter pixel count (WMPC)

Fig. 3 shows average age-related WMPC values across the four slices of the three indices (FA, Prob and Disp) for TD participants and the study group. As can be gleaned from Fig. 3, in normal individuals, changes continue throughout adulthood, approaching asymptotic values well into the third decade of life. Comparing the data of children with autism to the normal curve, there was a significant *increase* in the percent of pixels with mature white matter values in all three indices relative to age matched TD controls (FA: $t(6)=2.59$, $p=0.02$; Prob: $t(6)=2.47$, $p=0.024$; Disp: $t(6)=4.55$, $p=0.001$).

ROI analysis

Fig. 4 presents mean values of FA, Prob and Disp for each ROI. Recall that increase in FA/Prob values and decrease in Disp values indicate increased restriction. Significant increase in FA and Prob and decrease in Disp values were detected in the study group in the following regions: plic-left, ec-left and fminor-left. Prob was increased and Disp was decreased in the following regions: alic-left and -right, fminor-right and cst-left in slice 3. FA values were increased in the gcc, scc and cst-left in slice 2. Increase in Prob
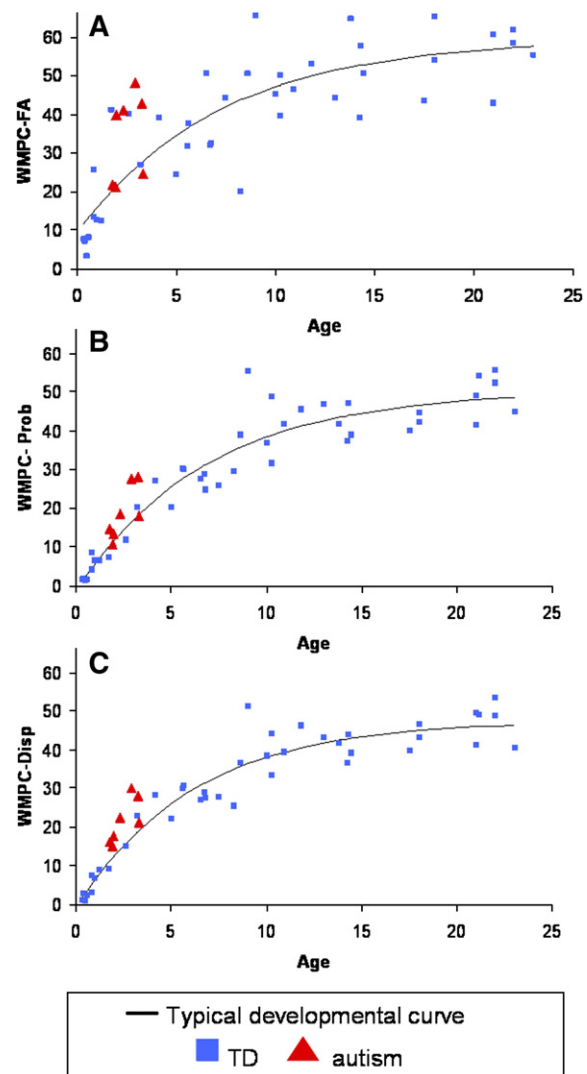

Fig. 3. White matter pixel count (WMPC) fractional anisotropy (FA—A), probability (Prob—B) and displacement (Disp—C). Individual values of typically developing (TD) controls and children with autism are plotted against the predicted developmental curve.
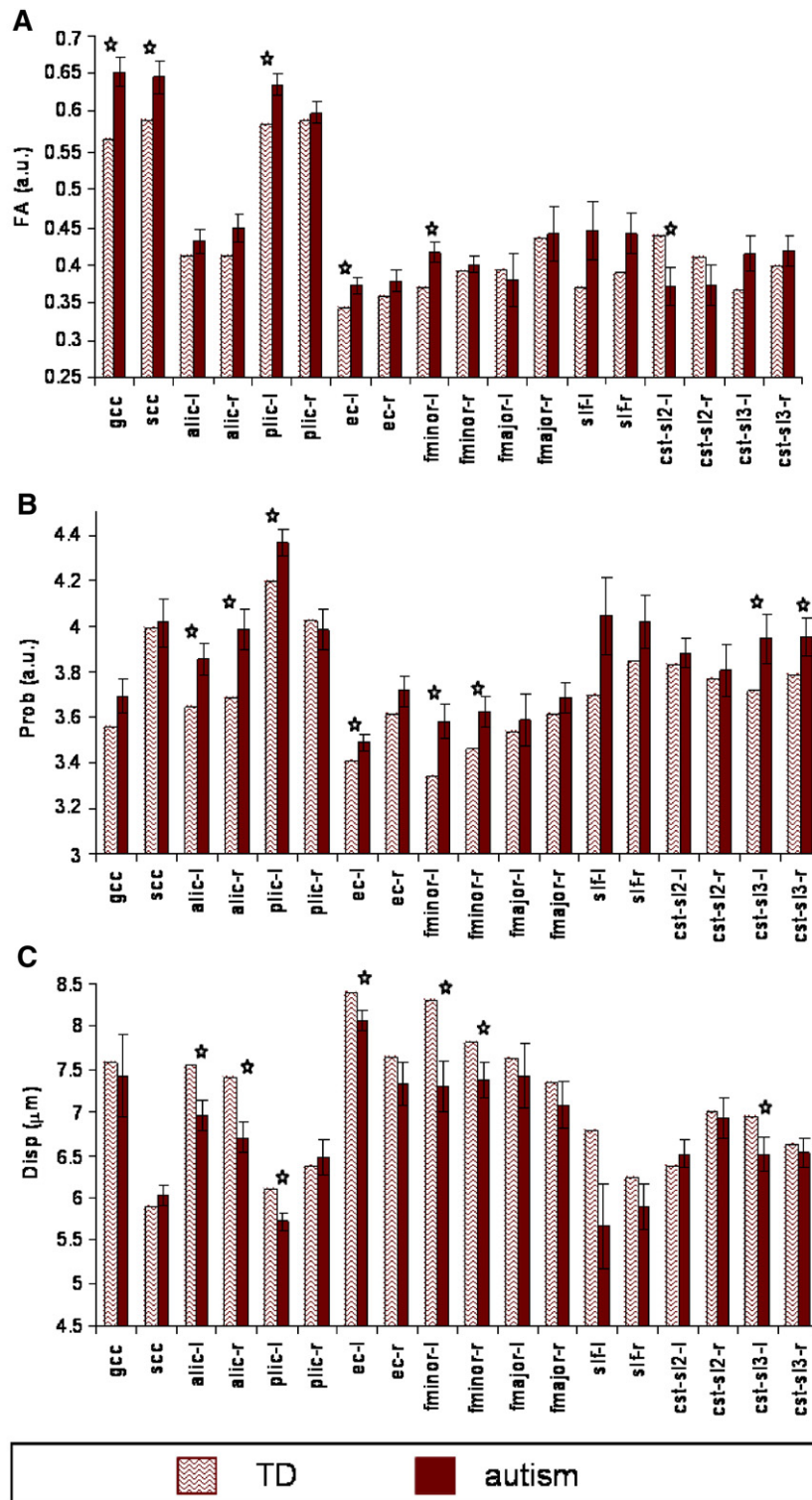
Fig. 4. Mean values of fractional anisotropy (FA—A), probability (Prob—B) and displacement (Disp—C) from all ROIs. *$p < 0.033$. TD: typically developing controls; gcc: genu of the corpus callosum; scc: splenium of the corpus callosum; alic: anterior limb of the internal capsule; plic: posterior limb of the internal capsule; ec: external capsule; fminor: forceps minor; fmajor: forceps major; slf: superior longitudinal fasciculus; cst: cortico-spinal tracts; l: left; r: right; a.u.: arbitrary units; μm: micrometer.

value was detected in the cst-right in slice 3. Increase in FA and Prob and decrease in Disp values approached significance ($p \leq 0.05$) in the left-slf region, but not in the right-slf. Thus,

statistically significant differences between ROIs indicated *higher* restriction except for the lower FA values observed on the left cst on slice 2.
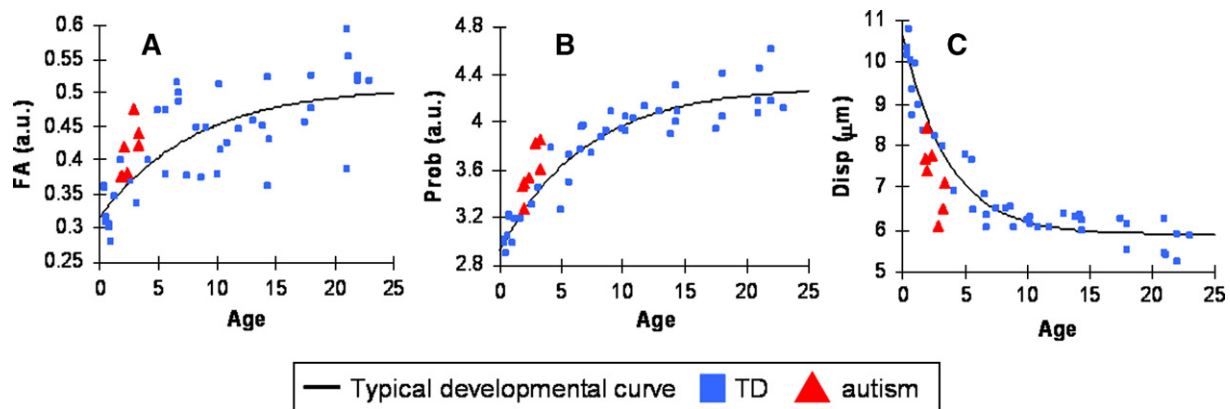
Fig. 5. Data obtained from the left fminor region. Developmental curves were obtained using minimal regression analysis. Values of fractional anisotropy (FA), probability (Prob) and displacement (Disp) in typically developing (TD) controls and in children with autism are plotted against the developmental curves (A–C).

Fig. 5 shows developmental curves for the fminor. Fig. 6 shows developmental curves for the fmajor. Importantly, the frontal fminor area but not the posterior fmajor area shows increased restriction.

Discussion

Based on DTI and high b value DWI, our findings demonstrate increased restricted diffusion in white matter in overall analysis (WMPC) as well as in selected ROIs in young children with confirmed diagnosis of autism, ages 1.8–3.3. This work presents the first evidence of accelerated maturation of white matter and provides quantitative information regarding white matter integrity in young children with autism. Although small, the study group was homogenous in age as well as in clinical status. Children had no neurological co-morbidities and were under the age of 4, which is the critical age for which brain overgrowth has been reported.

These findings add to the converging evidence of accelerated brain growth in autism in the first 2–4 years of life (Aylward et al., 2002; Courchesne et al., 2001; Courchesne and Pierce, 2005; Lainhart, 2006; Redcay and Courchesne, 2005). Note that previous DTI studies which reported *reduced* FA in frontal white matter and

in the corpus callosum in autism (Alexander et al., 2006; Barnea-Goraly et al., 2004; Keller et al., 2006; Lazar et al., 2006) were conducted with adolescents and adults, in whom brain growth is supposedly arrested (Penn, 2006; Redcay and Courchesne, 2005).

The current results are in line with Williams et al. (2006) report of an increase in ADC values in the arcuate fasciculus in young children with autism. However, in this abstract Williams did not report differences in FA, whereas such differences were detected in the current study. Our ability to detect differences in FA values may be due to the fact that FA values in our study were extracted from high b value data sets, so that long TE of 128 ms was used, as compared to most studies of low b value where TE of about 95–97 ms was used. FA values under these conditions were sensitive to white matter changes in healthy controls over a longer developmental period and allowed a comparison of this trend with the autistic group.

As can be gleaned from Figs. 4–6, significantly higher restriction was found in the study group in both hemispheres in the anterior fminor area, but not in the posterior fmajor area. Such findings of abnormal frontal vs. normal posterior white matter values are compatible with reports of increased white matter volume detected in the frontal but not in the occipital lobes in autism (Courchesne and Pierce, 2005). Furthermore, these results
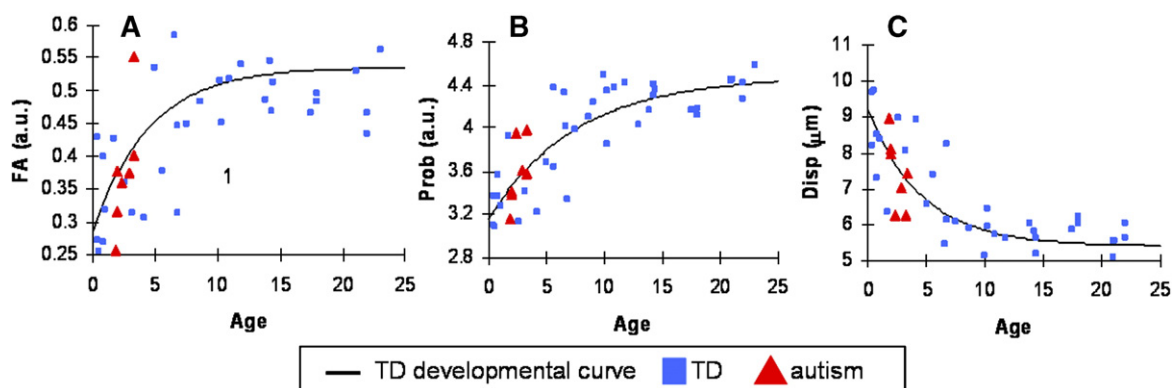

Fig. 6. Data obtained from the left posterior fmajor region. Developmental curves were obtained using minimal regression analysis. Values of fractional anisotropy (FA), probability (Prob) and displacement (Disp) in typically developing (TD) controls and in children with autism are plotted against the developmental curves (A–C).

tie in with claims that pre- and postnatal development proceed from posterior to anterior brain regions (Barkovitch, 1996; Kinney et al., 1988). Posterior–anterior developmental progression is reflected in the current results as well, in the starting point and asymptotic values of the estimated normal curves that indicate a higher degree of maturation in the posterior vs. anterior area. If indeed the frontal areas are slow maturing, they are likely to be more vulnerable to postnatal abnormalities that may relate to deficits in high cognitive functioning and social behavior in autism.

Our results bear upon the controversy surrounding hemispheric differences in autism. Hazlett et al. (2006) reported significant increase in gray matter volume in the left frontal and temporal lobes of subjects with autism (age 13–29), while Herbert et al. (2004) reported widespread rightward cerebral cortical asymmetry in high functioning autism (ages 5.7–11.3; Herbert et al., 2005). In the current study, increased restriction was detected in the left posterior/external limb of the internal capsule and in the left cortico-spinal tract in the third slice. Similar differences were not detected in ROIs in the right hemisphere. Our results indicate maturational disturbances that are more dominant in the left hemisphere. Those might be expressed later in life in abnormal lateral preference in various motor and language tasks.

In addition to the left asymmetry found in the abovementioned regions, in the left slf, differences indicating increase in restriction were close to significant ($p \leq 0.05$, where significance level was at $p = 0.033$). Such differences were not detected in the right slf. The slf is a major white matter bundle associated with language that connects the frontal temporal and parietal lobes. Earlier work suggested that in healthy controls, there was an increase in white matter volumes and in FA in the left slf as compared to the right-slf (Nucifora et al., 2005; Powell et al., 2006). Such differences are thought to reflect the left lateralization of the language function. The differences observed in our study may therefore relate to the language faculty in children with autism.

The current results leave open the question whether increased restriction in autism at this young age is due to increase in number, size of axons or myelination processes, or whether it is the result of reduced synaptic pruning early in development (Eigsti and Shapiro, 2003; McCaffery and Deutsch, 2005). Furthermore, it is not clear whether this is a primary or a secondary process of neuronal or columnar alteration.

Finally, whereas the results suggest accelerated maturation of white matter in autism, pilot studies of children with CP and PDD-NOS showed *decreased* diffusion and hence under-maturation. Similarly, a study of FA in children with developmental delays showed reduced FA in white matter when compared to neuro-developmentally healthy children (Filippi et al., 2003). Thus, it is possible that over-restriction distinguishes children with autism from other developmental disorders. Given that over-restriction is detectable at a young age, it might contribute to the early diagnosis of autism. To answer these questions, further studies using advanced imaging methods that will compare children with autism to children with other disabilities are needed.

Acknowledgments

References

Akshoomoff, N., Lord, C., Lincoln, A.J., Courchesne, R.Y., Carper, R.A., Townsend, J., Courchesne, E., 2004. Outcome classification of preschool children with autism spectrum disorders using MRI brain measures. J. Am. Acad. Child Adolesc. Psych. 43, 349–357.

Alexander, A.L., Lee, J.E., Lazar, M., Boudos, R., Dubray, M.B., Oakes, T.R., Miller, J.N., Lu, J., Jeong, E.K., McMahon, W.M., Bigler, E.D., Lainhart, J.E., 2007. Diffusion tensor imaging of the corpus callosum in autism. NeuroImage 34 (1), 61–73.

Assaf, Y., Cohen, Y., 2000. Assignment of the water slow-diffusing component in the central nervous system using q-space diffusion MRS: implications for fiber tract imaging. Magn. Reson. Med. 43, 191–199.

Assaf, Y., Ben-Bashat, D., Chapman, J., Peled, S., Biton, I.E., Kafri, M., Segev, Y., Hendler, T., Korczyn, A.D., Graif, M., Cohen, Y., 2002a. High b-value q-space analyzed diffusion-weighted MRI: application to multiple sclerosis. Magn. Reson. Med. 47, 115–126.

Assaf, Y., Mayzel-Oreg, O., Gigi, A., Ben-Bashat, D., Mordohovitch, M., Verchovsky, R., Reider, I.I.G., Hendler, T., Graif, M., Cohen, Y., Korczyn, A.D., 2002b. High b value q-space-analyzed diffusion MRI in vascular dementia: a preliminary study. J Neurol Sci 203–204, 235–239.

Aylward, E.H., Minshew, N.J., Field, K., Sparks, B.F., Singh, N., 2002. Effects of age on brain volume and head circumference in autism. Neurology 59, 175–183.

Barkovitch, A.J., 1996. Pediatric Neuroimaging. Lippincott-Raven, Philadelphia, NY.

Barnea-Goraly, N., Kwon, H., Menon, V., Eliez, S., Lotspeich, L., Reiss, A.L., 2004. White matter structure in autism: preliminary evidence from diffusion tensor imaging. Biol. Psychiatry 55, 323–326.

Basser, P.J., Mattiello, J., LeBihan, D., 1994. Estimation of the effective self-diffusion tensor from the NMR spin echo. J. Magn. Reson., B 103, 247–254.

Ben-Bashat, D., Ben Sira, L.G., Graif, M., Pianka, P., Hendler, T., Cohen, Y., Assaf, Y., 2003. White matter maturation from birth through adulthood: high b value diffusion weighted imaging study. Structural MRI in Psychiatry. Psychiatr. Neuroimaging 348, 39–43.

Ben-Bashat, D., Ben Sira, L.G., Graif, M., Pianka, P., Hendler, T., Cohen, Y., Assaf, Y., 2004. Advanced MR methods in adrenoleukodystrophy. Proceedings of the 12th Annual Meeting of ISMRM, Kyoto, Japan.

Ben Bashat, D., Ben Sira, L., Graif, M., Pianka, P., Hendler, T., Cohen, Y., Assaf, Y., 2005. Normal white matter development from infancy to adulthood: comparing diffusion tensor and high b value diffusion weighted MR images. J. Magn. Reson. Imaging 21, 503–511.

Ben-Itzchak, E., Zachor, D.A., 2007. The effects of intellectual functioning and autism severity on outcome of early behavioral intervention for children with autism. Res. Dev. Disabil. 28 (3), 287–303.

Bertrand, J., Mars, A., Boyle, C., Bove, F., Yeargin-Allsopp, M., Decoufle, P., 2001. Prevalence of autism in a United States population: the Brick Township, New Jersey, investigation. Pediatrics 108, 1155–1161.

Carper, R.A., Courchesne, E., 2005. Localized enlargement of the frontal cortex in early autism. Biol. Psychiatry 57, 126–133.

Carper, R.A., Moses, P., Tigue, Z.D., Courchesne, E., 2002. Cerebral lobes in autism: early hyperplasia and abnormal age effects. NeuroImage 16, 1038–1051.

Casanova, M.F., Buxhoeveden, D.P., Brown, C., 2002a. Clinical and macroscopic correlates of minicolumnar pathology in autism. J. Child Neurol. 17, 692–695.

Casanova, M.F., Buxhoeveden, D.P., Switala, A.E., Roy, E., 2002b. Minicolumnar pathology in autism. Neurology 58, 428–432.

Courchesne, E., Pierce, K., 2005. Brain overgrowth in autism during a critical time in development: implications for frontal pyramidal neuron

and interneuron development and connectivity. Int. J. Dev. Neurosci. 23, 153–170.

Courchesne, E., Karns, C.M., Davis, H.R., Ziccardi, R., Carper, R.A., Tigue, Z.D., Chisum, H.J., Moses, P., Pierce, K., Lord, C., Lincoln, A.J., Pizzo, S., Schreibman, L., Haas, R.H., Akshoomoff, N.A., Courchesne, R.Y., 2001. Unusual brain growth patterns in early life in patients with autistic disorder: an MRI study. Neurology 57, 245–254.

Eigsti, I.M., Shapiro, T., 2003. A systems neuroscience approach to autism: biological, cognitive, and clinical perspectives. Ment. Retard. Dev. Disabil. Res. Rev. 9, 205–215.

Engelbrecht, V., Scherer, A., Rassek, M., Witsack, H.J., Modder, U., 2002. Diffusion-weighted MR imaging in the brain in children: findings in the normal brain and in the brain with white matter diseases. Radiology 222, 410–418.

Filippi, C.G., Lin, D.D., Tsiouris, A.J., Watts, R., Packard, A.M., Heier, L.A., Ulug, A.M., 2003. Diffusion-tensor MR imaging in children with developmental delay: preliminary findings. Radiology 229, 44–50.

Fombonne, E., 2003. Epidemiological surveys of autism and other pervasive developmental disorders: an update. J. Autism Dev. Disord. 33, 365–382.

Hazlett, H.C., Poe, M.D., Gerig, G., Smith, R.G., Piven, J., 2006. Cortical gray and white brain tissue volume in adolescents and adults with autism. Biol. Psychiatry 59, 1–6.

Herbert, M.R., Ziegler, D.A., Makris, N., Filipek, P.A., Kemper, T.L., Normandin, J.J., Sanders, H.A., Kennedy, D.N., Caviness Jr., V.S., 2004. Localization of white matter volume increase in autism and developmental language disorder. Ann. Neurol. 55, 530–540.

Herbert, M.R., Ziegler, D.A., Deutsch, C.K., O'Brien, L.M., Kennedy, D.N., Filipek, P.A., Bakardjiev, A.I., Hodgson, J., Takeoka, M., Makris, N., Caviness Jr., V.S., 2005. Brain asymmetries in autism and developmental language disorder: a nested whole-brain analysis. Brain 128, 213–226.

Hermoye, L., Saint-Martin, C., Cosnard, G., Lee, S.K., Kim, J., Nassogne, M.C., Menten, R., Clapuyt, P., Donohue, P.K., Hua, K., Wakana, S., Jiang, H., van Zijl, P.C., Mori, S., 2006. Pediatric diffusion tensor imaging: normal database and observation of the white matter maturation in early childhood. NeuroImage 29, 493–504.

Just, M.A., Cherkassky, V.L., Keller, T.A., Minshew, N.J., 2004. Cortical activation and synchronization during sentence comprehension in high-functioning autism: evidence of underconnectivity. Brain 127, 1811–1821.

Kinney, H.C., Brody, B.A., Kloman, A.S., Gilles, F.H., 1988. Sequence of central nervous system myelination in human infancy: II. Patterns of myelination in autopsied infants. J. Neuropathol. Exp. Neurol. 47, 217–234.

Lainhart, J.E., 2006. Advances in autism neuroimaging research for the clinician and geneticist. Am. J. Med. Genet. C. Semin. Med. Genet. 142, 33–39.

Lord, C., Rutter, M., Le Couteur, A., 1994. Autism Diagnostic Interview-Revised: a revised version of a diagnostic interview for caregivers of individuals with possible pervasive developmental disorders. J. Autism Dev. Disord. 24, 659–685.

Lord, C., Rutter, M., DiLavore, P.C., Risi, S., 1999. Autism Diagnostic Observation Schedule-WPS (ADOS-WPS). Western Psychological Services, Los Angeles.

Lord, C., Risi, S., Lambrecht, L., Cook Jr., E.H., Leventhal, B.L., DiLavore, P.C., Pickles, A., Rutter, M., 2000. The autism diagnostic observation schedule-generic: a standard measure of social and communication deficits associated with the spectrum of autism. J. Autism Dev. Disord. 30, 205–223.

McCaffery, P., Deutsch, C.K., 2005. Macrocephaly and the control of brain growth in autistic disorders. Prog. Neurobiol. 77, 38–56.

McGraw, P., Liang, L., Provenzale, J.M., 2002. Evaluation of normal age-related changes in anisotropy during infancy and childhood as shown by diffusion tensor imaging. AJR Am. J. Roentgenol. 179, 1515–1522.

Mendelsohn, A., Strous, R.D., Bleich, M., Assaf, Y., Hendler, T., 2006. Regional axonal abnormalities in first episode schizophrenia: preliminary evidence based on high b-value diffusion-weighted imaging. Psychiatry Res. 146, 223–229.

Minshew, N.J., Goldstein, G., Siegel, D.J., 1997. Neuropsychologic functioning in autism: profile of a complex information processing disorder. J. Int. Neuropsychol. Soc. 3, 303–316.

Mori, S., Wakana, S., Nagae-Postscher, L.M., van Zijl, P.C.M., 2005. MRI Atlas of Human White Matter. Elsevier B.V, Amsterdam.

Mukherjee, P., McKinstry, R.C., 2006. Diffusion tensor imaging and tractography of human brain development. Neuroimaging Clin. N. Am. 16 (19–43), vii.

Mukherjee, P., Miller, J.H., Shimony, J.S., Philip, J.V., Nehra, D., Snyder, A.Z., Conturo, T.E., Neil, J.J., McKinstry, R.C., 2002. Diffusion-tensor MR imaging of gray and white matter development during normal human brain maturation. AJNR Am. J. Neuroradiol. 23, 1445–1456.

Neil, J., Miller, J., Mukherjee, P., Huppi, P.S., 2002. Diffusion tensor imaging of normal and injured developing human brain—A technical review. NMR Biomed. 15, 543–552.

Nucifora, P.G., Verma, R., Melhem, E.R., Gur, R.E., Gur, R.C., 2005. Leftward asymmetry in relative fiber density of the arcuate fasciculus. NeuroReport 16, 791–794.

Pajevic, S., Pierpaoli, C., 1999. Color schemes to represent the orientation of anisotropic tissues from diffusion tensor data: application to white matter fiber tract mapping in the human brain. Magn. Reson. Med. 42, 526–540.

Penn, H.E., 2006. Neurobiological correlates of autism: a review of recent research. Neuropsychol. Dev. Cogn., C. Child Neuropsychol. 12, 57–79.

Powell, H.W., Parker, G.J., Alexander, D.C., Symms, M.R., Boulby, P.A., Wheeler-Kingshott, C.A., Barker, G.J., Noppeney, U., Koepp, M.J., Duncan, J.S., 2006. Hemispheric asymmetries in language-related pathways: a combined functional MRI and tractography study. NeuroImage 32, 388–399.

Redcay, E., Courchesne, E., 2005. When is the brain enlarged in autism? A meta-analysis of all brain size reports. Biol. Psychiatry 58, 1–9.

Sparks, B.F., Friedman, S.D., Shaw, D.W., Aylward, E.H., Echelard, D., Artru, A.A., Maravilla, K.R., Giedd, J.N., Munson, J., Dawson, G., Dager, S.R., 2002. Brain structural abnormalities in young children with autism spectrum disorder. Neurology 59, 184–192.

Unpublished

Keller, T.A., Kana, R.K., Minshew, R.K., Just, M.A., 2006. Reduced fractional anisotropy in high functioning adults with autism localizes to meaningful regions of white matter. 5th International Meeting For Autism Research (IMFAR), Montreal, Canada, 1–3 June 2006, pp. 78–79.

Lazar, M., Baxter, B., Alexander, A., Oakes, T., Bigler, E., Lainhart, J., 2006. A diffusion tensor imaging study of the thalamus in autism. 5th International Meeting for Autism Research (IMFAR), Montreal, Canada, 1–3 June 2006, pp. 23–24.

Williams, M.T., Eluvathingal, T.J., Behen, M.E., Chugani, M.E., Chugani, H.T., 2006. Abnormal asymmetry in the arcuate fasciculus of autistic children: A DTI study. 5th International Meeting For Autism Research (IMFAR), Montreal, Canada, 1–3 June 2006, pp. 79.